Scapula development is governed by genetic interactions of *Pbx1* with its family members and with *Emx2* via their cooperative control of *Alx1*

Terence D. Capellini[1],*, Giulia Vaccari[2],*, Elisabetta Ferretti[1], Sebastian Fantini[2], Mu He[1], Massimo Pellegrini[3], Laura Quintana[4], Giuseppina Di Giacomo[1], James Sharpe[4,5], Licia Selleri[1,†] and Vincenzo Zappavigna[2,†]

SUMMARY

The genetic pathways underlying shoulder blade development are largely unknown, as gene networks controlling limb morphogenesis have limited influence on scapula formation. Analysis of mouse mutants for Pbx and *Emx2* genes has suggested their potential roles in girdle development. In this study, by generating compound mutant mice, we examined the genetic control of scapula development by Pbx genes and their functional relationship with *Emx2*. Analyses of Pbx and *Pbx1;Emx2* compound mutants revealed that Pbx genes share overlapping functions in shoulder development and that *Pbx1* genetically interacts with *Emx2* in this process. Here, we provide a biochemical basis for *Pbx1;Emx2* genetic interaction by showing that Pbx1 and Emx2 can bind specific DNA sequences as heterodimers. Moreover, the expression of genes crucial for scapula development is altered in these mutants, indicating that Pbx genes act upstream of essential pathways for scapula formation. In particular, expression of *Alx1*, an effector of scapula blade patterning, is absent in all compound mutants. We demonstrate that Pbx1 and Emx2 bind in vivo to a conserved sequence upstream of *Alx1* and cooperatively activate its transcription via this potential regulatory element. Our results establish an essential role for *Pbx1* in genetic interactions with its family members and with *Emx2* and delineate novel regulatory networks in shoulder girdle development.

KEY WORDS: Emx2, Girdle, Hox, Pbx, Mouse, Scapula

INTRODUCTION

The development of the shoulder blade (scapula) is poorly understood. In the chick, its proximal components, i.e. the blade and spine, derive from dermomyotomal mesenchyme, whereas its distal components, i.e. the glenoid cavity and coracoid, as well as the acromion, derive partly from the somatopleuric compartment of the lateral plate mesoderm (LPM) (Huang et al., 2000; Wang et al., 2005) (see Fig. 2). In the mouse, the bony structures of the scapula have dual neural crest-mesoderm origin, as shown by genetic lineage labeling (Matsuoka et al., 2005).

Scapula development is modestly affected by the genetic pathways that pattern the limb (e.g. Prahlad et al., 1979; Ros et al., 1996), and there is only rudimentary knowledge of the genes that act upstream of blade and head development (Huang et al., 2006). By contrast, much information has been gathered on genes that finely pattern these structures. For example, *Pax1/Hoxa5* and *Hoxc6* are involved in acromion and head development, respectively (Aubin et al., 1998; Timmons et al., 1994). Additionally, two distinct pathways have been suggested in blade

patterning (Kuijper et al., 2005): one regulated by *Emx2*, the loss-of-function of which results in blade absence in mice (Pellegrini et al., 2001), and the other governed by genetic interactions among *aristaless*-related (*Alx1*, *Alx3*, *Alx4*), T-box (*Tbx15*) and Gli (*Gli3*) genes. It remains unknown whether these two blade-specific pathways are separate or integrated, whether *Emx2* controls one or both, and which genes act upstream of *Emx2* in blade and head morphogenesis.

Recent studies suggest that Pbx TALE homeoproteins control scapula development (Capellini et al., 2006; Selleri et al., 2001). Indeed, *Pbx1*-null (*Pbx1*^{−/−}) embryos exhibit hypoplastic blades and scapular head-humeral fusions (Selleri et al., 2001), whereas compound *Pbx1*^{−/−};*Pbx2*^{+/−} mutants present exacerbations of these phenotypes (Capellini et al., 2006; Capellini et al., 2008). Conversely, the single loss of *Pbx2* or *Pbx3* does not cause scapula mutant phenotypes (Rhee et al., 2004; Selleri et al., 2004). Scapula and proximal limb have thus been proposed to be 'Pbx dependent', consistent with Pbx roles as Hox co-factors (reviewed by Moens and Selleri, 2006). However, loss of Hox genes, including entire Hox clusters, from pre-scapular tissues results, at best, in negligible scapula alterations, despite co-expression of Pbx and Hox genes in these domains (Fromental-Ramain et al., 1996; Aubin, 1997). Therefore, it currently appears unlikely that Pbx proteins function as Hox co-factors in scapula formation, suggesting instead cooperation with other factors.

Emx2 shares structural characteristics with Hox proteins, including: (1) a Gln (Q) in position 50 of the homeodomain, which is predicted to confer DNA-binding properties similar to those of Hox proteins; and (2) a YPWL sequence N-terminal to the homeodomain that resembles part of the Hox IYPWMK motif ['hexapeptide' (Bürglin, 1994)], a hallmark for heterodimerization

[1]Department of Cell and Developmental Biology, Weill Medical College of Cornell University, 1300 York Avenue, New York, NY 10021, USA. [2]Department of Animal Biology, University of Modena and Reggio-Emilia, Via Campi, 41100 Modena, Italy. [3]Department of Biomedical Sciences, University of Modena and Reggio-Emilia, Via Campi, 41100 Modena, Italy. [4]EMBL-CRG Systems Biology Unit, CRG, Dr Aiguader, 88, 08003 Barcelona, Spain. [5]ICREA Research Professor, 08010 Barcelona, Spain.

*These authors contributed equally to this work
†Authors for correspondence (lis2008@med.cornell.edu; zappavigna.vincenzo@unimore.it)

with Pbx (reviewed by Moens and Selleri, 2006). It has never been addressed, though, whether Pbx factors and Emx2 interact genetically and/or physically in scapula development.

Here, we demonstrate that Pbx genes share overlapping functions in scapula development, as *Pbx1;Pbx2* and *Pbx1;Pbx3* compound mutants display more severe and novel phenotypes compared with those of *Pbx1*$^{-/-}$ embryos. We also show that the expression of genes crucial for scapular blade patterning or acromion and head development is altered in these mutants, placing Pbx genes upstream of pathways involved in scapula ontogeny. Additionally, we demonstrate that *Pbx1* genetically interacts with *Emx2* in blade and spine formation, as compound *Pbx1;Emx2* mutants display novel defects. Moreover, we establish that Pbx1 and Emx2 heterodimerize on a specific DNA sequence, providing a molecular basis for their genetic interaction. Pbx1 and Emx2 proteins also bind in vivo to a conserved sequence upstream of the *Alx1* (formerly *Cart1*) gene, and cooperatively activate transcription via this potential regulatory element. Our results thus delineate novel genetic networks in shoulder girdle development.

MATERIALS AND METHODS
Mice
Intercrosses between *Pbx1*$^{+/-}$ (Selleri et al., 2001), *Pbx2*$^{+/-}$ (Selleri et al., 2004), *Pbx3*$^{+/-}$ (Rhee et al., 2004) and *Emx2*$^{+/-}$ (Pellegrini et al., 2001) mice were performed to obtain *Pbx1*$^{+/-}$;*Pbx2*$^{+/-}$, *Pbx1*$^{+/-}$;*Pbx3*$^{+/-}$, *Pbx2*$^{+/-}$;*Pbx3*$^{+/-}$ and *Pbx1*$^{+/-}$;*Emx2*$^{+/-}$ mutants. On a C57BL/6 background, the double-heterozygous numbers obtained were below the expected Mendelian ratios. To increase numbers, C57BL/6 double-heterozygous males for each mutant line were crossed to Black-Swiss [NIH-BL(S)]. Next, double-heterozygous C57BL/6 females and mixed double-heterozygous C57BL/6-Black-Swiss males were intercrossed and their progeny analyzed for skeletal phenotypes. On mixed genetic backgrounds, marked ameliorations of C57BL/6 scapular phenotypes were observed, which led us to use C57BL/6 to Black-Swiss intercrosses. To generate more complex Pbx compound genotypes, *Pbx1*$^{+/-}$;*Pbx2*$^{+/-}$ and *Pbx1*$^{+/-}$;*Pbx3*$^{+/-}$ mutants were intercrossed to obtain *Pbx1*$^{+/-}$;*Pbx2*$^{+/-}$;*Pbx3*$^{+/-}$ mice; their in utero lethality prevented further intercrossing.

Skeletal preparations, in situ hybridization, cell proliferation and apoptosis immunohistochemistry and optical projection tomography (OPT)
Skeletons of E13.5-14.5 embryos were stained with Alcian Blue/Alizarin Red S (Depew et al., 1999; McLeod, 1980). Whole-mount in situ hybridizations were performed on somite-matched embryos using digoxygenin-labeled RNA probes (Di Giacomo et al., 2006). *Alx1* (Kuijper et al., 2005), *Alx4* (Beverdam and Meijlink, 2001), *Emx2* (Pellegrini et al., 2001), *En1* (Davidson et al., 1988), *Gli3* (Beverdam and Meijlink, 2001), *Hoxc6* (Sharpe et al., 1988), *Pax1* (Chalepakis et al., 1991), *Pbx1* (Brendolan et al., 2005), *Pbx2* (Selleri et al., 2004), *Pbx3* (Di Giacomo et al., 2006), *Sox9* (Wright et al., 1995) and *Tbx15* (Kuijper et al., 2005) probes were used. Section in situ hybridization was conducted as described (Di Giacomo et al., 2006). Cell proliferation and apoptosis assays were carried out as described (Capellini et al., 2008); for details, see Fig. S1 in the supplementary material. Skeletal preparations and whole-mount in situ hybridization embryos were processed for OPT according to published protocols (Sharpe, 2003; Sharpe et al., 2002).

Chromatin immunoprecipitation (ChIP)
As previously described (Salsi et al., 2008), chromatin was extracted from mouse proximal forelimb and flank dissected from wild-type E11.5 embryos. Cross-linked chromatin was immunoprecipitated with 5 μg anti-Pbx antiserum (C-20, Santa Cruz) or a specific anti-Emx2 monoclonal antibody (see below). Semi-quantitative PCR analysis was performed on three independent ChIPs for each genomic region analyzed, and primers were designed accordingly (Salsi and Zappavigna, 2006) (see Table S1 in the supplementary material).

Plasmid constructs
The pSG5Pbx1 and pETPbx1 expression constructs for the Pbx1a protein have been described (Di Rocco et al., 1997). The pSG5Emx2 expression construct was generated by cloning *Eco*RI/*Bgl*II-cut PCR-amplified *Emx2* coding sequence into *Eco*RI/*Bam*HI-cut pSG5 (Stratagene) vector. The pRSETEmx2 expression construct was generated by cloning the *Emx2* coding sequence as an *Eco*RI fragment into the *Eco*RI site of the pRSETB vector. The pML(EP)$_6$ reporter construct was obtained by cloning a tandem hexamer of the EP oligonucleotide 5′-GATCCGTCGACGGATCAT-TAAAGCCCTCGAGA-3′ into the *Bgl*II site of the pML luciferase reporter (Di Rocco et al., 1997). The pML*Alx1*-EPBS(900) reporter was generated by cloning a 974 bp fragment containing the PCR-amplified *Alx1* 5′-7 genomic sequence [–4670 to –3699, relative to the transcription start site (TSS)] into the *Sma*I site of pML. The pML*Alx1*-EPBS reporter was generated by cloning a 130 bp PCR-amplified fragment from the *Alx1* 5′-7 region containing Sites A, B and C of the EPBS sequence (–4270 to –4139) into the *Nhe*I/*Bgl*II sites of pML. The pML*Alx1*-EPBS(900)A+Bmut and pML*Alx1*-EPBS mutated reporters (Amut, Bmut or Cmut) were obtained by mutating Site A, B, A+B or C within the EPBS element by PCR-mediated mutagenesis and cloning the fragments into the *Nhe*I/*Bgl*II sites of pML. The mutations were identical to those of the electrophoretic mobility shift assay (EMSA) oligonucleotide probes (see below). All PCR-amplified fragments were verified by sequencing.

Protein production and purification, binding site selection, cell extracts and EMSAs
His-tagged Emx2 and Pbx1 proteins were produced in *E. coli* using pRSETEmx2 and pETPbx1 plasmids and purified using Ni-NTA Agarose (Qiagen). For binding site selection, purified Emx2 and Pbx1 proteins were incubated with ^{32}P-labeled SelEP oligonucleotide pool (5′-GGCGA-GATCTCTCGAGGGNNNNNATGATCCGTCGACGGATCCGCGG-3′) in binding buffer (Chang et al., 1995) for 30 minutes at 0°C and electrophoresed on a 6% polyacrylamide gel in 0.5× TBE. The retarded band corresponding to the Emx2-Pbx1 heterodimer was excised and eluted in 0.5 M ammonium acetate, 10 mM MgCl$_2$, 1 mM EDTA, 0.1% SDS. Aliquots of the eluted band were PCR amplified for 30 cycles (95°C 1 minute, 55°C 30 seconds, 72°C 1 minute) with primers complementary to the flanking arms of SelPE, and the amplified DNA was used in further binding reactions. After six selection rounds, amplified DNA was cloned, sequenced and consensus sequences were aligned using CLUSTAL W (Thompson et al., 1994) (http://workbench.sdsc.edu).

EMSAs were performed (Di Rocco et al., 2001) using purified, bacterially produced Emx2 and Pbx1 proteins, or whole-cell extracts (10-20 μg each) from COS cells exogenously expressing both genes. To identify protein-DNA complexes, 200 ng of anti-Pbx antibody (C20, Santa Cruz) or 0.1 μl of an anti-Emx2 monoclonal antibody were added to binding reactions, which were separated by 6% PAGE in 0.5× TBE, dried and exposed to film. The anti-Emx2 monoclonal antibody was generated using the N-terminal portion of Emx2 and tested for its lack of cross-reaction with Pbx1 by immunoblotting. Oligonucleotides used in EMSAs were (mutated nucleotides are underlined):

Alx1-EPBS, 5′-TATAGCTTTGATGTAAGTAGAAGTATCTTTCATG-TCCAAAATTAAAATTACATT-3′;

EPBS-Amut, 5′-TATAGC<u>GGGGCGGGC</u>AGTAGAAGTATCTTTCA-TGTCCAAAATTAAAATTACATT-3′;

EPBS-Bmut, 5′-TATAGCTTTGATGTAAGTAGAAGTATCT<u>GGACG</u>-GTCCAAAATTAAAATTACATT-3′; and

EPBS-Cmut, 5′-TATAGCTTTGATGTAAGTAGAAGTATCTTTCA-TGTCCAAA<u>CGGC</u>AA<u>CGGC</u>CATT-3′.

Cell culture, transfections and luciferase assays
P19 mouse embryonal carcinoma cells were cultured in MEMα with 10% foetal calf serum. In typical transfections, performed by CaPO$_4$ precipitation, reporter plasmid (5 μg), protein expression construct (2-4 μg), pCH110 β-galactosidase plasmid (0.5 μg) as an internal control, and pBluescript (variable quantities), were added to a total of 20 μg transfected DNA per 9-cm dish. Cells were harvested 48 hours post-transfection, and assayed for luciferase and β-galactosidase expression (Zappavigna et al., 1994).

RESULTS

Pbx genes are co-expressed in prospective scapular-forming domains

At E10.5, *Pbx1* and *Pbx2*, but not *Pbx3*, were expressed in the dermomyotome and somatopleure (see Fig. S1A in the supplementary material). However, from E11 to E12, all three Pbx genes were detected, although *Pbx3* was at lower levels (see Fig. S1B in the supplementary material). At E10.5-11.5, all three Pbx genes were co-expressed in proximal forelimb mesenchyme (Fig. 1A,C), corroborating previous reports (Capellini et al., 2006). This pattern persisted until E11.0-11.5, when the expression of *Pbx1* remained proximal, whereas *Pbx3* was confined to proximal-anterior limb domains and *Pbx2* to distal domains (see Capellini et al., 2006; Di Giacomo et al., 2006). *Emx2* was co-expressed with Pbx genes at E10.5 (Fig. 1A,C) (Theil et al., 1999; Tian and Lev, 2002).

Pbx1 genetically interacts with *Pbx2* and *Pbx3* to form scapular structures

Given the overlapping expression of the Pbx genes in pre-scapular domains, compound Pbx mutants were generated to investigate the respective contributions of *Pbx1-3*. Scapula defects were evident in only three allelic combinations: $Pbx1^{-/-}$, $Pbx1^{-/-};Pbx2^{+/-}$ and $Pbx1^{-/-};Pbx3^{+/-}$ (Fig. 2A,C; see Fig. S2A in the supplementary material); $Pbx1^{-/-};Pbx2^{-/-}$ and $Pbx1^{-/-};Pbx3^{-/-}$ mutants died in utero before scapula morphogenesis (Capellini et al., 2006).

At E13.5, $Pbx1^{-/-}$ embryos exhibited reduced blades and spines, obliterated glenoid cavities fused to humeral heads and expanded coracoids (Fig. 2A) (Selleri et al., 2001). In $Pbx1^{-/-};Pbx2^{+/-}$ mutants (Pbx1/2Mut), several $Pbx1^{-/-}$ scapula phenotypes were exacerbated and novel defects became evident. Cartilage preparations at E12.5 revealed that scapular condensations were disorganized and reduced, indicating disruption prior to mesenchyme formation (Capellini et al., 2006). Analysis of *Sox9* expression, a mesenchymal condensation marker, revealed significant reductions across the superior-to-inferior blade-forming domains (Fig. 3A). OPT (Sharpe, 2003; Sharpe et al., 2002) of the three-dimensional expanse of *Sox9* expression revealed a decrease in mesenchyme across entire pre-scapular domains (Fig. 3C; see Fig. S2B and Movie 1 in the supplementary material). As a result, reduced cartilages were observed at E12.5/E13.5 in skeletal preparations and by OPT. Pbx1/2Mut scapulae (Fig. 2A,C; see Fig. S2A and Movie 2 in the supplementary material) were dysmorphic, their blades were markedly reduced compared with those of $Pbx1^{-/-}$ and wild-type (WT) embryos, and their only intact aspects were near the head-neck junction. Furthermore, spines and acromia were absent. The remaining 'scapular' mass was fused to the humeral head with an adjoining skeletal element, possibly a duplicated scapular/humeral head (Fig. 2A, inset, Fig. 2C; see Fig. S2A in the supplementary material). At E13.5, skeletal preparations and OPT revealed that $Pbx1^{-/-};Pbx3^{+/-}$ (Pbx1/3Mut) embryos also exhibited scapulae with proximal-to-distal blade reductions (Fig. 2A,C; see Fig. S2A in the supplementary material), although less severe than in Pbx1/2Mut embryos (Fig. 2A,C; see Fig. S2A and Movie 3 in the supplementary material). Additionally, Pbx1/3Mut scapulae showed blade indentations (Fig. 2C; see Fig. S2A in the supplementary material) and foramina (Fig. 2A), lacked well-developed spines and acromia, and their heads remained fused to humeri and were potentially duplicated (Fig. 2A,C; see Fig. S2A in the supplementary material). *Sox9* expression was reduced in Pbx1/3Mut scapular domains (Fig. 3A; see Fig. S2B in the
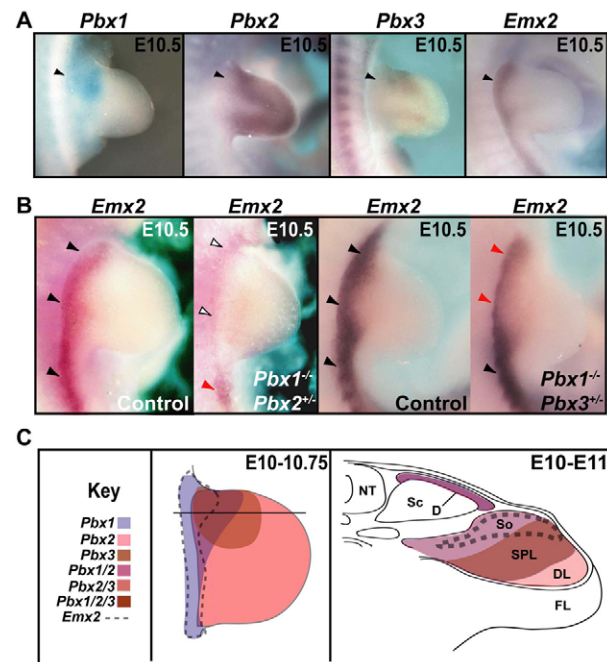
supplementary material), although OPT revealed that this reduction was not as drastic as in Pbx1/2Mut embryos (Fig. 3C; see Fig. S2B and Movie 4 in the supplementary material).

Scapular domains of *Pbx2;Pbx3* mutants, particularly $Pbx2^{-/-};Pbx3^{+/-}$ and $Pbx2^{+/-};Pbx3^{-/-}$ embryos, appeared similar to those of WT (not shown), whereas $Pbx2^{-/-};Pbx3^{-/-}$ mutants died before shoulder development could be assessed (i.e. before E10.5). Finally, *Pbx1;Pbx2;Pbx3* compound mutants could not be obtained owing to the perinatal lethality of $Pbx1^{+/-};Pbx2^{+/-};Pbx3^{+/-}$ embryos, which did not exhibit appendicular defects (not shown).

Pbx1 genetically interacts with *Emx2* during scapular blade formation

In light of the blade defects of compound Pbx mutants, we examined the expression of *Emx2*, the absence of which results in blade agenesis (Pellegrini et al., 2001). Whereas *Emx2* was unchanged in E10.5 $Pbx1^{-/-}$ embryos (not shown), it was severely and moderately reduced in Pbx1/2Mut and Pbx1/3Mut embryos, respectively (Fig. 1B). By contrast, *Pbx1-3* expression remained grossly unperturbed in the proximal-superior forelimbs of $Emx2^{-/-}$ embryos (see Fig. S1C in the supplementary material).

Given that (1) Pbx and *Emx2* genes are co-expressed in blade-patterning domains, (2) mice deficient for either of these genes exhibit blade phenotypes, and (3) both Pbx and Emx2 proteins
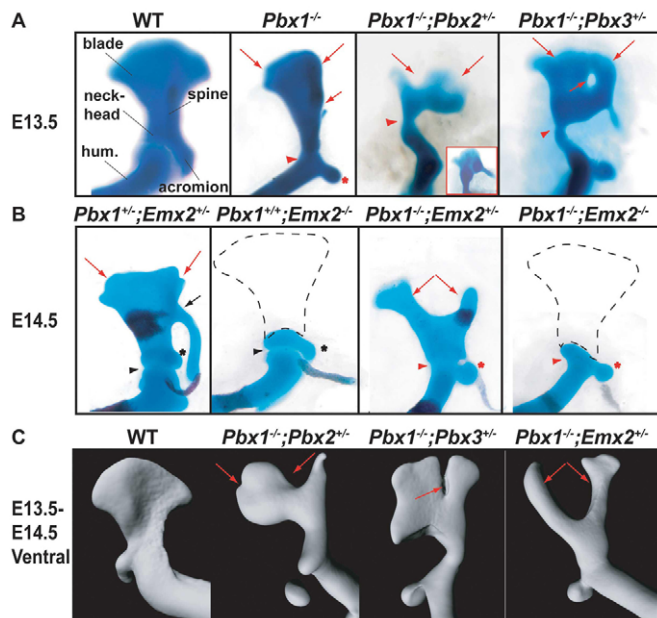

Fig. 1. Expression of Pbx and *Emx2* genes in pre-scapular domains in wild-type mice and Pbx compound mutants. Expression was assessed by in situ hybridization. (**A**) *Pbx1-3* and *Emx2* co-expression in wild-type (WT) E10.5 proximal-superior forelimbs. (**B**) *Emx2* expression in E10.5 Pbx compound mutants. Compared with WT (black arrowheads), *Emx2* is severely reduced in $Pbx1^{-/-};Pbx2^{+/-}$ (white arrowheads) and reduced in $Pbx1^{-/-};Pbx3^{+/-}$ forelimbs (red arrowheads), but present in posterior flank mesoderm (black arrowheads). (**C**) Diagram of *Pbx1-3* and *Emx2* co-expression in E10-10.75 proximal limbs (left) and in a transverse section at the superior forelimb level in an E10-11 WT embryo. The differently shaded domains and dashed lines represent overlapping expression territories for *Pbx1-3* and *Emx2*.

Fig. 2. Hard-tissue phenotypes of compound Pbx and *Pbx1;Emx2* mutants. Phenotypes were assessed in mutants versus WT littermates by skeletal preparation and OPT. (**A**) E13.5 *Pbx1⁻/⁻* scapulae exhibit blade dysmorphologies (long red arrows), shortened spines (short red arrow), head-humeral fusions (red arrowhead) and coracoid expansions (red asterisk). *Pbx1⁻/⁻;Pbx2⁺/⁻* scapulae exhibit proximal-distal blade reductions (long red arrows), whereas *Pbx1⁻/⁻;Pbx3⁺/⁻* have blade indentations (long red arrows) and foramina (short red arrow). Both mutants show scapular-humeral joint fusions (red arrowhead), potential head duplications (inset) and coracoid dysmorphologies. (**B**) E14-14.5 *Pbx1⁺/⁻;Emx2⁺/⁻* scapulae exhibit proximal blade indentations/reductions (red arrows), whereas *Pbx1⁺/⁺;Emx2⁻/⁻* embryos lack blades (dashed black line) but retain coracoids (black asterisk) and scapular-humeral joints (black arrowhead). *Pbx1⁻/⁻;Emx2⁺/⁻* embryos exhibit bifurcated blades (red arrows). *Pbx1⁻/⁻;Emx2⁻/⁻* exhibit blade absence (dashed line), and scapular-humeral joint fusions (red arrowhead) and coracoid malformations (red asterisk). (**C**) As assessed by OPT, *Pbx1⁻/⁻;Pbx2⁺/⁻* embryos display reduced blades along their central/lateral domains (red arrows), *Pbx1⁻/⁻;Pbx3⁺/⁻* embryos show reduced blades with proximal-to-distal indentations (red arrow) and *Pbx1⁻/⁻;Emx2⁺/⁻* embryos show blade bifurcations with rami appearing as rounded long bones (red arrows).

Fig. 3. Mesenchymal phenotypes of compound *Pbx1-3* and *Pbx1;Emx2* mutants. Phenotypes were assessed by *Sox9* in situ hybridization and OPT. (**A**) In specific E12.25 pre-scapular domains, *Sox9* expression is reduced in *Pbx1⁻/⁻* (red arrowheads), significantly reduced in *Pbx1⁻/⁻;Pbx2⁺/⁻* (white arrowheads), and reduced in *Pbx1⁻/⁻;Pbx3⁺/⁻* (red and white arrowheads) embryos. (**B**) In E12.25 pre-scapular domains, *Sox9* expression is normal in *Pbx1⁺/⁻;Emx2⁺/⁻* (black arrowheads), slightly reduced in *Pbx1⁻/⁻;Emx2⁺/⁻* (red arrowheads) and severely reduced (double red arrowheads) to nearly absent (white arrowheads) in *Pbx1⁺/⁺;Emx2⁻/⁻* embryos. (**C**) OPT of *Sox9* expression at E12.25. Dorsal views of *Sox9* OPT in the pre-scapular domains outlined by red dashed boxes in A and B reveal reductions in blade mesenchyme in *Pbx1⁻/⁻;Pbx2⁺/⁻* (red arrowheads), less severe reductions with indentations in *Pbx1⁻/⁻;Pbx3⁺/⁻* (red arrowheads), and strong central vertebral reductions in *Pbx1⁻/⁻;Emx2⁺/⁻* (double red arrowheads) embryos. The asterisk in *Pbx1⁻/⁻;Pbx2⁺/⁻* indicates expanded/duplicated humeral heads.

possess structural features permitting their heterodimerization, potential genetic interactions of *Pbx1* with *Emx2* were assessed. At E14.5, *Pbx1⁺/⁺;Emx2⁻/⁻* embryos displayed blade loss, as previously reported (Fig. 2B) (Pellegrini et al., 2001), whereas *Pbx1⁻/⁻;Emx2⁺/⁺* embryos exhibited blade alterations and head fusions (Fig. 2A) (Selleri et al., 2001). Genetic interaction was evident in *Pbx1⁺/⁻;Emx2⁺/⁻* embryos, which showed minor proximal blade reductions that were absent in single *Pbx1⁺/⁻* or *Emx2⁺/⁻* progeny (not shown), and in *Pbx1⁻/⁻;Emx2⁺/⁻* mutants (Pbx1/Emx2Mut), which exhibited centrally bifurcated blades with superior and inferior rami resembling individual bones (Fig. 2B). OPT uniquely revealed rounded, shaft-like rami, rather than flattened, blade-like structures (Fig. 2C; see Fig. S2A and Movie 5 in the supplementary material). These phenotypes were not observed in *Pbx1⁻/⁻* or *Emx2⁺/⁻* embryos (Fig. 2B,C). Additionally, Pbx1/Emx2Mut limbs displayed scapular-humeral head fusions, as in *Pbx1⁻/⁻* mutants (Fig. 2B,C; see Fig. S2A in the supplementary
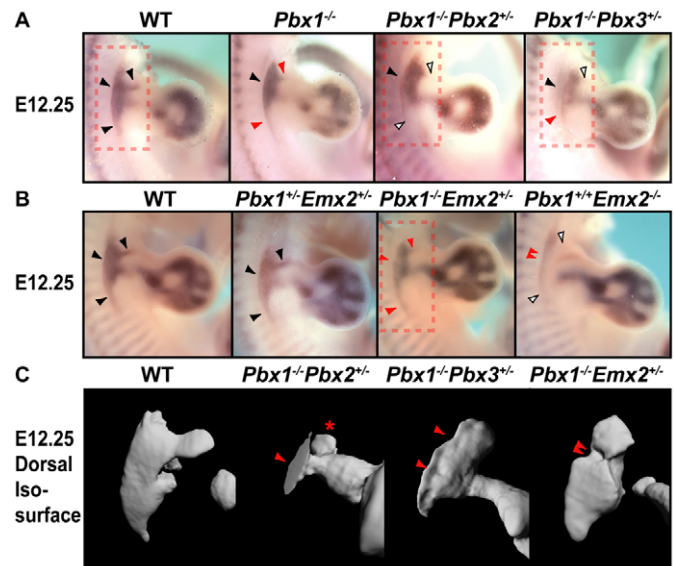
material) (Selleri et al., 2001). Analysis of *Sox9* expression in Pbx1/Emx2Mut embryos at E12.5 revealed reduced mesenchymal condensations, and OPT revealed this mesenchyme to be markedly indented along its vertebral border, foreshadowing later scapular bifurcation (Fig. 3C; see Fig. S2B and Movie 6 in the supplementary material). Finally, *Pbx1⁻/⁻;Emx2⁻/⁻* mutants displayed blade agenesis, as in *Emx2⁻/⁻* embryos, and scapular-humeral head fusions, as in *Pbx1⁻/⁻* embryos (Fig. 2B). Given the additive phenotype of *Pbx1⁻/⁻;Emx2⁻/⁻* mutants, only Pbx1/Emx2Mut mice were studied for scapula marker gene expression.

Pbx factors are required for the expression of genes involved in scapular head formation

To investigate Pbx and *Emx2* roles in patterning distal scapular structures, the expression of genes crucial for head and acromial development was examined in compound mutants. *Pax1*, a regulator of acromion formation (Aubin et al., 2002; Timmons et al., 1994; Wilm et al., 1998), was markedly reduced proximally (Fig. 4A, left) but was maintained within its dorsoventral domain (Fig. 4B, left) in Pbx1/2Mut and Pbx1/3Mut embryos, whereas it was only slightly decreased in *Pbx1⁻/⁻* mutants (Fig. 4A, left). Severe reductions were not present in *Emx2⁻/⁻* or Pbx1/Emx2Mut embryos (Fig. 4A, left). Although *Hoxc6⁻/⁻* mutants lack scapular
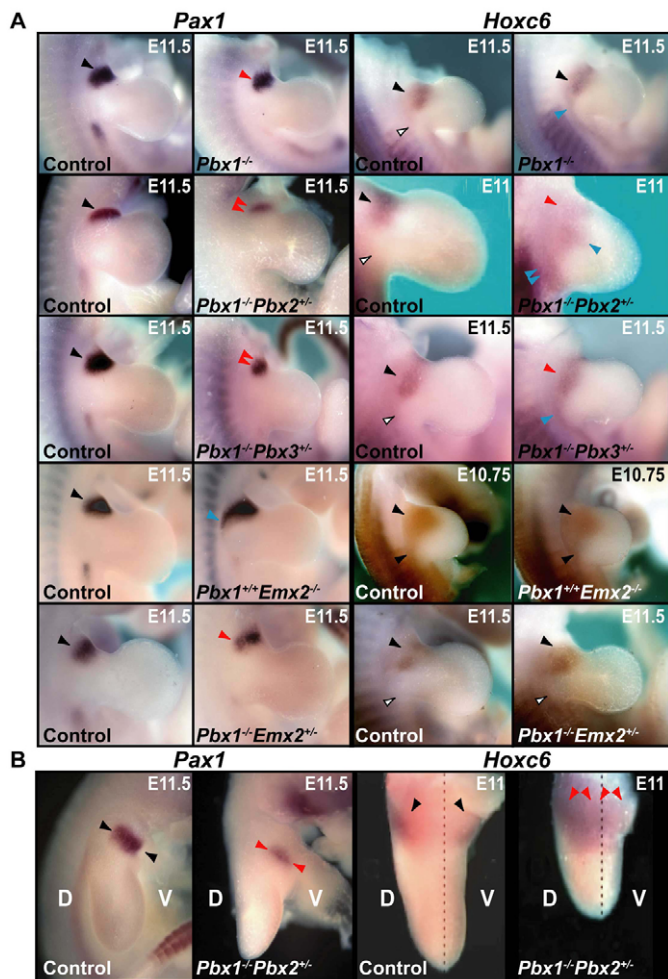
Fig. 4. Expression of acromion and head markers in E11.5 compound Pbx and *Pbx1;Emx2* mutants. Expression was assessed by in situ hybridization. (**A**) Compared with controls (black arrowheads), *Pax1* expression (left panels) is reduced in *Pbx1⁻/⁻* and *Pbx1⁻/⁻;Emx2⁺/⁻* (red arrowheads), markedly reduced in *Pbx1⁻/⁻;Pbx2⁺/⁻* and *Pbx1⁻/⁻;Pbx3⁺/⁻* (double red arrowheads) and proximally expanded in *Pbx1⁺/⁺;Emx2⁻/⁻* (blue arrowhead) mutants. Compared with controls (black and white arrowheads), *Hoxc6* expression (right panels) is expanded in *Pbx1⁻/⁻* and *Pbx1⁻/⁻;Pbx3⁺/⁻* (blue arrowheads), drastically expanded in *Pbx1⁻/⁻;Pbx2⁺/⁻* (double blue arrowheads) and unchanged in *Pbx1⁺/⁺;Emx2⁻/⁻* and *Pbx1⁻/⁻;Emx2⁺/⁻* (black arrowheads) mutants at E10.75/E11.5. (**B**) In *Pbx1⁻/⁻;Pbx2⁺/⁻* embryos, *Pax1* expression (left panels) remains dorsoventrally restricted (red arrowheads) within the normal domain (black arrowheads). *Hoxc6* (right panels) is dorsoventrally expanded across the midline of the forelimb (dashed line) in *Pbx1⁻/⁻;Pbx2⁺/⁻* (red arrowheads) compared with WT (black arrowheads) embryos. Magnification of WT and *Pbx1⁻/⁻;Pbx2⁺/⁻ Hoxc6* panels is 1.5× that of the other panels. D, dorsal; V, ventral.

head malformations (Garcia-Gasca and Spyropoulos, 2000), misexpression studies implicate this gene in its specification (Oliver et al., 1990). In *Pbx1⁻/⁻*, Pbx1/2Mut and Pbx1/3Mut embryos, *Hoxc6* was posteriorly expanded in limbs, unlike in controls (Fig. 4A, right) and was dorsoventrally expanded in compound Pbx mutants (Fig. 4B, right), but unaltered in *Emx2⁻/⁻* or Pbx1/Emx2Mut embryos (Fig. 4A, right).

Pbx factors and Emx2 are required for the expression of genes involved in blade patterning

Only the proximal forelimb expression of regulators of blade patterning was considered crucial (Fig. 5; see Figs S3 and S4 in the supplementary material), as distal domains typically correlate with limb development (Huang et al., 2006). The expression of *Alx1*, a gene that patterns the superior blade (Kuijper et al., 2005), was reduced in *Pbx1⁻/⁻* (Fig. 5A, left) and *Emx2⁻/⁻* (see Fig. S3 in the supplementary material) proximal forelimbs, whereas it was absent in E10.5-11.5 Pbx1/2Mut, Pbx1/3Mut and Pbx1/Emx2Mut proximal forelimbs (Fig. 5A, left). At E10.5, the expression of *Alx4*, which also patterns the superior blade, was only slightly reduced in *Pbx1⁻/⁻* and Pbx1/Emx2Mut proximal forelimbs, but markedly reduced and spatially altered in Pbx1/2Mut and Pbx1/3Mut forelimbs (Fig. 5A, right). However, this perturbation was not as extreme at E11.5 in all mutants (see Fig. S4 in the supplementary material), including *Emx2⁻/⁻* mutants (see Fig. S3 in the supplementary material). Expression of *Tbx15*, a gene that patterns the central blade, was only reduced in Pbx1/2Mut proximal forelimbs at E10.5 (Fig. 5B, left), whereas at E11.5 it was expanded in proximal forelimbs of *Pbx1⁻/⁻* embryos and all other mutants lacking *Pbx1* (see Fig. S4 in the supplementary material) but was absent in *Emx2⁻/⁻* mutants (see Fig. S3 in the supplementary material). Expression of *Gli3*, which patterns the inferior blade, was nearly absent and reduced in Pbx1/2Mut and Pbx1/3Mut proximal forelimbs, respectively, from E10.5 (Fig. 5B, right) through E11.5, when only Pbx1/Emx2Mut (see Fig. S4 in the supplementary material) and *Emx2⁻/⁻* (see Fig. S3 in the supplementary material) embryos retained normal *Gli3* expression. The expression of *Gli3* and *Alx4*, along with engrailed 1 (*En1*), which demarcates the somitic dermomyotome (Davidson et al., 1988), was unaltered in all of these mutants (not shown). These results are summarized in Fig. 8A.

Finally, proliferation and apoptosis assays were carried out in Pbx1/2Mut and Pbx1/Emx2Mut embryos (see Fig. S5 in the supplementary material; data not shown). No marked differences in cell proliferation, as assessed by in vivo BrdU incorporation, and in apoptosis, as revealed by anti-caspase 3 immunohistochemistry, were identified in pre-scapular domains of Pbx1/2Mut versus WT embryos from E9.5 to E11.5 (see Fig. S5A in the supplementary material; data not shown). Similarly, there was no conspicuous increase in apoptosis in Pbx1/Emx2Mut embryos (data not shown). By contrast, Pbx1/Emx2Mut embryos displayed reductions in cell proliferation compared with WT (see Fig. S5B in the supplementary material), and more marked reductions were observed in *Emx2⁻/⁻* embryos, which lack the blade altogether (Pellegrini et al., 2001).

Emx2 and Pbx1 can form stable DNA-bound, transcriptionally active heterodimers

Given the *Emx2* and *Pbx1* genetic interaction, we determined the as yet unexplored optimal DNA-binding consensus sequence for a putative Emx2-Pbx1 heterodimer. An oligonucleotide containing random nucleotides in the five positions 5′ to the Pbx1 TGAT core consensus binding sequence (Lu et al., 1995; Van Dijk et al., 1993), along with purified Emx2 and Pbx1 proteins, were used in site-selection experiments (see Materials and methods). Emx2 and Pbx1 proved to bind DNA as a heterodimer, preferentially to sites matching the consensus sequence 5′-CTTTAATGAT-3′ (hereafter, the 'EP' binding site) (not shown). To confirm that Emx2 and Pbx1 cooperatively bind EP, EMSAs were performed using whole-cell extracts from COS cells exogenously expressing Emx2 or Pbx1, alone or in combination. Extracts containing both Emx2 and Pbx1
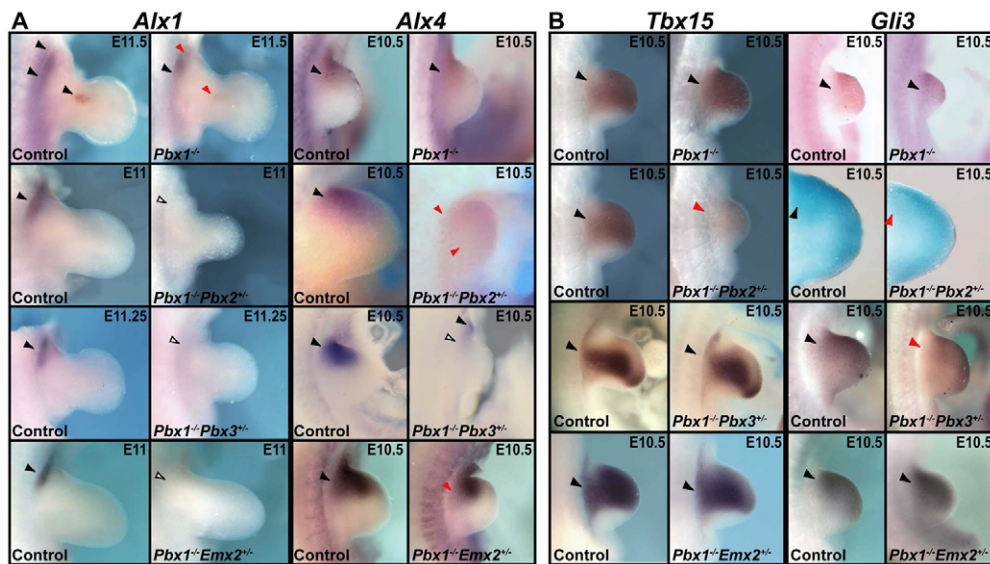
Fig. 5. Expression of blade-patterning genes in E10.5-11.5 compound Pbx and *Pbx1;Emx2* mutants. Expression was compared in mutants and control littermates (black arrowheads) by in situ hybridization. (**A**) (Left) *Alx1* is reduced in *Pbx1*$^{-/-}$ (red arrowheads) and is undetected in *Pbx1*$^{-/-}$;*Pbx2*$^{+/-}$, *Pbx1*$^{-/-}$;*Pbx3*$^{+/-}$ and *Pbx1*$^{-/-}$;*Emx2*$^{+/-}$ (white arrowheads) mutants. (Right) *Alx4* expression remains normal in *Pbx1*$^{-/-}$ (black arrowheads), whereas it is markedly (red arrowheads) and severely (white arrowheads) reduced in *Pbx1*$^{-/-}$;*Pbx2*$^{+/-}$ and *Pbx1*$^{-/-}$;*Pbx3*$^{+/-}$ mutants, respectively. In *Pbx1*$^{-/-}$;*Emx2*$^{+/-}$ forelimbs, *Alx4* is only slightly reduced (red arrowhead). (**B**) (Left) *Tbx15* is markedly reduced only in *Pbx1*$^{-/-}$;*Pbx2*$^{+/-}$ proximal forelimbs (red arrowhead). (Right) *Gli3* is normal in *Pbx1*$^{-/-}$ and *Pbx1*$^{-/-}$;*Emx2*$^{+/-}$ (black arrowheads), whereas it is markedly reduced in *Pbx1*$^{-/-}$;*Pbx2*$^{+/-}$ (red arrowhead) and slightly reduced in *Pbx1*$^{-/-}$;*Pbx3*$^{+/-}$ (red arrowhead) proximal-superior forelimbs. Magnification of *Gli3* and *Alx4* expression in WT and *Pbx1*$^{-/-}$;*Pbx2*$^{+/-}$ panels is 2.5× that of other panels.

showed a retarded band (Fig. 6A, lane 8) that was supershifted or abolished by the addition of an anti-Emx2 or anti-Pbx1 antibody, respectively (Fig. 6A, lanes 9 and 10). Whereas Pbx1 alone did not bind the EP site (lanes 5 and 6), Emx2 alone formed a faster-migrating shifted complex (lanes 3 and 4).

To test whether Emx2 and Pbx1 activate transcription via the EP site, a luciferase reporter construct containing six EP copies upstream of the adenovirus major late (AdML) minimal promoter [pML(EP)$_6$] (Fig. 6B) was transiently transfected into P19 embryonal carcinoma cells with increasing amounts of *Emx2* and/or *Pbx1* expression constructs. Whereas Emx2 or Pbx1 alone could not activate transcription via EP, their co-expression led to a significant stimulation above reporter basal activity (Fig. 6B), indicating that they physically interact to form DNA-bound heterodimers on specific DNA sequences and cooperatively activate transcription.

Emx2 and Pbx1 bind the *Alx1* locus in vivo and cooperatively activate transcription via a conserved *Alx1* upstream element

As *Emx2* and *Pbx1* act upstream of *Alx1* (Fig. 5A, left), we examined whether *Alx1* transcription is directly regulated by Emx2 and/or Pbx1. We searched for EP consensus sequences within a region spanning from ~10 kb 5′ to the putative *Alx1* transcription start site (TSS) to ~20 kb 3′ to its polyadenylation signal (PAS), using MatInspector (Cartharius et al., 2005; Quandt et al., 1995). A binding site matrix representing the EP consensus was generated using MatInd (Cartharius et al., 2005), based on our site-selection results (not shown). Because an evolutionarily conserved motif similar to the EP consensus was not identified within this region, we determined whether Emx2 and/or Pbx1 were bound in vivo to putative *Alx1* regulatory sequences. ChIP was performed on sixteen genomic regions surrounding *Alx1* exons, chosen because of their evolutionary conservation and gene proximity (Fig. 7A). Nine

regions were 5′ to the *Alx1* TSS, with the most upstream (5′-8) 9 kb away (Fig. 7A), and seven were 3′ to the *Alx1* PAS, with the most downstream (3′-7) 16 kb away (Fig. 7A). ChIP on E11.5 WT mouse proximal forelimb and flank chromatin using anti-Pbx and anti-Emx2 antibodies revealed that only region 5′-7 (Fig. 7A,B), comprising −4472 to −4075 from the TSS, displayed significant enrichments for both Emx2- and Pbx1-immunoprecipitated chromatin (Fig. 7B). This 400 bp region and its conserved flanking sequences were analyzed by EMSA for binding by Emx2 and Pbx1 (not shown). Only a highly conserved 54 bp sequence overlapping the 3′ end of this region showed significant binding (*Alx1*-EPBS, Fig. 7C). The *Alx1*-EPBS sequence was bound weakly by Pbx1 alone and not by Emx2 alone (Fig. 7D, left, lanes 2 and 3). However, addition of both Emx2 and Pbx1 led to the formation of a retarded band (Fig. 7D, lane 4) that was supershifted or abolished by an anti-Emx2 or anti-Pbx1 antibody, respectively (lanes 5 and 6), demonstrating that Emx2 and Pbx1 cooperatively bind *Alx1*-EPBS. The *Alx1*-EPBS sequence contains a conserved TGAT motif (Site A) representing the Pbx1 binding consensus, a conserved TCAT motif (Site B) found within the EP site (ATCATTAAAG, complementary strand), and two non-conserved ATTA motifs (Site C). We mutated (see Materials and methods) these three putative core binding motifs (EPBS-Amut, EPBS-Bmut and EPBS-Cmut, Fig. 7D) and tested them in EMSAs. Mutation of TGAT (Amut, lanes 7-10) or TCAT (Bmut, lanes 11-14) motifs strongly reduced Pbx1-Emx2 cooperative binding, whereas mutation of the ATTA motifs (Cmut, lanes 15-18) only weakly reduced the formation of the Pbx1-Emx2 retarded complex.

To test whether Pbx1 and/or Emx2 activated transcription via the *Alx1*-EPBS sequence, we generated luciferase reporter constructs by inserting a 974 bp fragment spanning region 5′-7 (Fig. 7A) including the *Alx1*-EPBS sequence [EPBS(900), Fig. 7E], or a 130 bp fragment that exclusively encompasses the *Alx1*-EPBS sequence (EPBS, Fig.
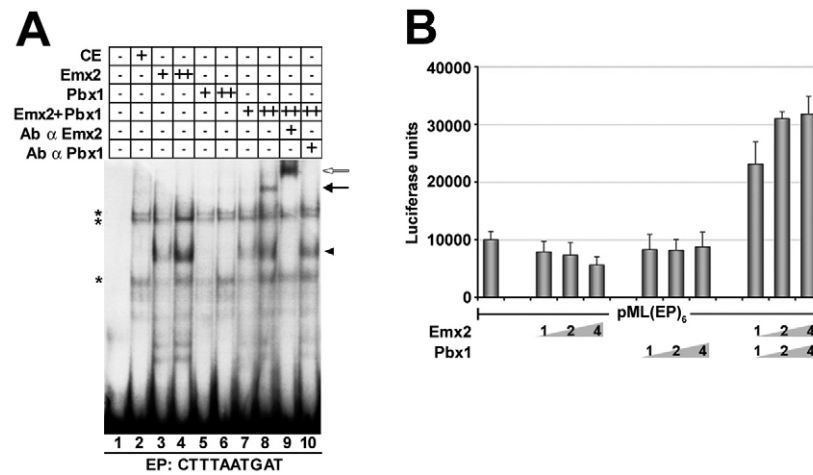
Fig. 6. Pbx and Emx2 physically interact and cooperatively regulate transcription in cell culture. (**A**) EMSA using an oligonucleotide representing the consensus binding sequence of Emx2-Pbx1 heterodimers (EP site). Whole-cell extracts (20 and 40 μg) were used from COS cells transiently transfected with expression vectors for Emx2 and/or Pbx1. Co-expressed Emx2 and Pbx1 led to the formation of a retarded band (black arrow, lane 8) that was supershifted (white arrow) or abolished by the addition of an anti-Emx2 (lane 9) or anti-Pbx1 (lane 10) antibody, respectively. CE, control whole-cell extract of non-transfected COS cells. Black arrowhead indicates binding of Emx2 alone to the probe. Asterisks indicate non-specific complexes. (**B**) Luciferase activity, in arbitrary units, assayed from P19 cell extracts transiently transfected with the pML(EP)$_6$ reporter, together with Pbx1 and/or Emx2 expression constructs. Numbers indicate amounts (μg) of transfected expression constructs. Bars represent mean luciferase activity ± s.e.m. of at least five independent experiments.

7E), upstream of the AdML promoter. These reporter constructs were transfected together with Emx2 and/or Pbx1 expression constructs into P19 cells. Whereas Emx2 and Pbx1 alone did not appreciably stimulate the EPBS(900), or the EPBS, reporter activity, their co-expression led to an increase in EPBS(900) (~5.9-fold) and EPBS (~5.4-fold) reporter activity (Fig. 7E). We then generated reporter constructs carrying the same mutations tested in EMSAs within the single Site A (EPBS-Amut), Site B (EPBS-Bmut) or Site C (EPBS-Cmut), and a compound mutation of Sites A and B [EPBS(900)A+Bmut] (Fig. 7E). Whereas the mutation of Site C did not cause any reduction in reporter transactivation by Emx2 and Pbx1, the mutation of Site A or Site B caused a decrease in reporter transactivation (Fig. 7E). A further decrease in Emx2-Pbx1-mediated transcriptional activation was caused by the compound mutation of Sites A and B (Fig. 7E). These results indicate that both Sites A and B are necessary for the assembly of a DNA-bound Emx2-Pbx1 complex and for full transcriptional activation by Emx2-Pbx1 via the *Alx1*-EPBS sequence, whereas Site C is dispensable.

DISCUSSION
Pbx genes control scapular blade and head development
In dermomyotome, in which *Pbx3* is not expressed, the compound absence of *Pbx1* and *Pbx2* does not alter the expression of scapular blade-patterning genes (e.g. *Gli3*, *Alx4*). Of note, although we previously reported rostral shifts in Hox gene expression in Pbx1/2Mut paraxial mesoderm (Capellini et al., 2006), no known single or compound Hox mutant displays blade defects. Only *Hox5* mutants exhibit rostral blade shifts, with normal blade morphology (Rancourt et al., 1995). Thus, we cannot yet invoke a mechanism whereby loss of Pbx proteins, as Hox co-factors, leads to the blade phenotypes of Pbx compound mutants via altered Hox function.

As in dermomyotome, the expression of *Pbx1-3* does not colocalize in somatopleure. However, they do show overlapping expression in limb mesoderm (Fig. 1A,C). Indeed, *Pbx1* and *Pbx2* show the most extensive overlapping expression in E8.0-10.5 LPM

and proximal limbs (Fig. 1C) (Capellini et al., 2006), whereas *Pbx1* and *Pbx3* colocalize only in proximal-anterior limbs after E9.5 and within somatopleure after E11.0 (Fig. 1) (Di Giacomo et al., 2006). Accordingly, blade defect severity in Pbx1/2Mut significantly exceeds that of Pbx1/3Mut embryos, and is supported by the accentuated reduction in blade-patterning gene expression in Pbx1/2Mut embryos (see below). These findings indicate that *Pbx2* is more crucial than *Pbx3* in scapular development, probably because it shares greater spatiotemporal domains with *Pbx1*, or is expressed at higher levels.

Importantly, most girdle and LPM limb derivatives are hypoplastic and malformed in compound Pbx mutants. Pbx1/2Mut and Pbx1/3Mut scapulae also exhibit markedly abnormal head morphologies. Analyses of known molecular markers of the head (*Hoxc6*) and acromion (*Pax1*) revealed that they are spatially diffused and reduced in these mutants, although they are still present in domains that lack detectable changes in cell proliferation and apoptosis. Furthermore, as *Pax1* and *Hoxc6* are reduced in their domains, other mesodermal genes such as *Tbx15* are upregulated. These findings corroborate our previous reports on the disruption of Hox expression in Pbx1/2Mut forelimbs (Capellini et al., 2006). For example, we reported the upregulation of *Hoxa9* and *Hoxd9*, genes that are involved in the growth and patterning of the stylopod in Pbx1/2Mut forelimbs (Capellini et al., 2006). Along with spatial expansions of other 3′ Hox genes (i.e. *Hoxc6*), such data support our finding of potential scapular head/humeral head duplications in these mutants (Fig. 8B). Thus, the hierarchical role of Pbx factors in Hox gene expression and/or their role as Hox co-factors in the LPM are likely mechanisms for assigning positional information to head progenitors.

Lastly, our results show that whereas *Pbx1;Pbx2* and *Pbx1;Pbx3* mutants exhibit severe blade and head defects, *Pbx2;Pbx3* mutants are normal. Therefore, in light of the overlapping functions of Pbx genes in development (Capellini et al., 2006; Capellini et al., 2008; Stankunas et al., 2008), we establish that the dosage of *Pbx1* is paramount also in scapula morphogenesis.
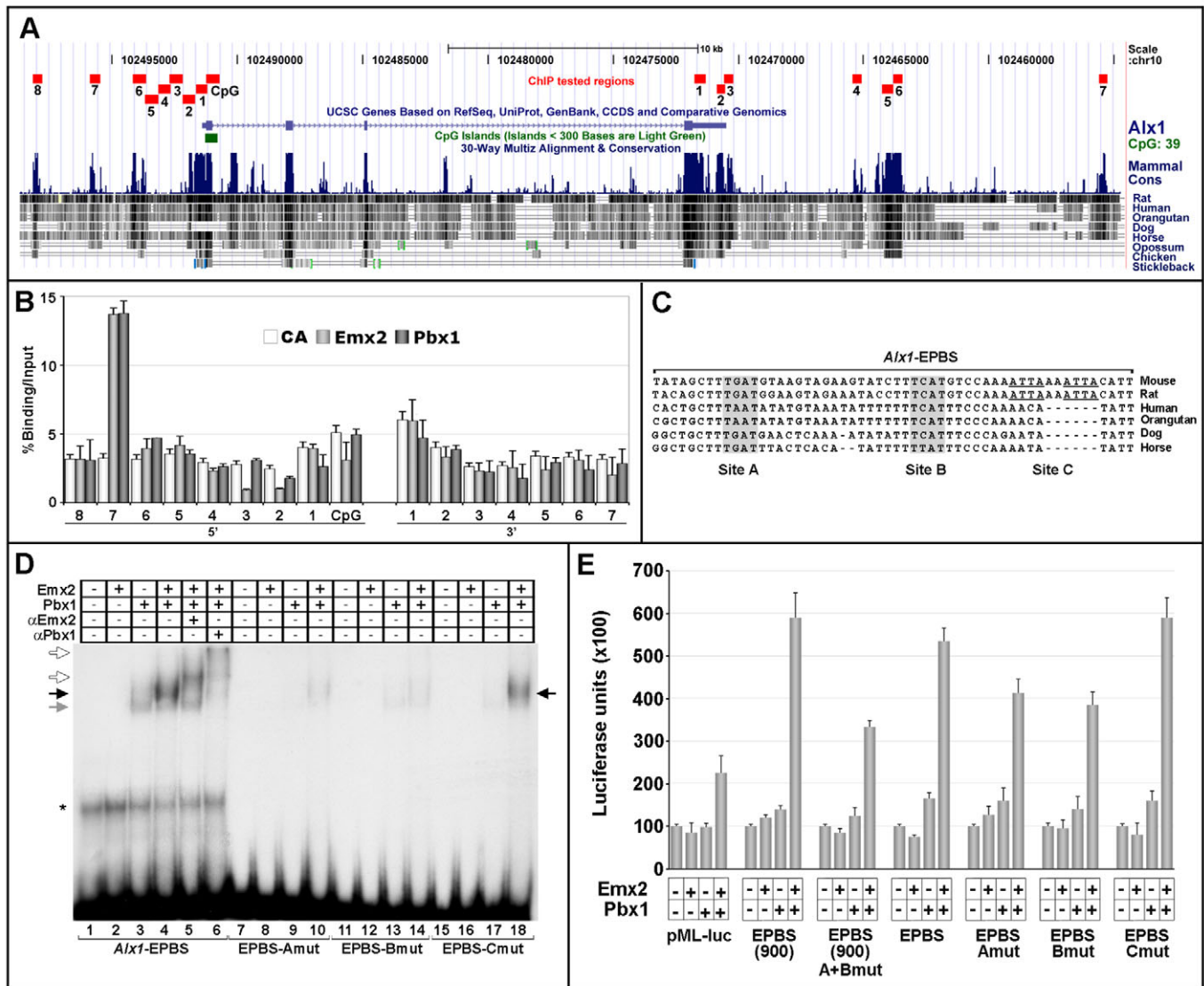
Fig. 7. Pbx and Emx2 bind in vivo and cooperatively regulate transcription at a putative *Alx1* regulatory element. (A) Interspecies comparison of genomic sequences spanning ~25 kb around *Alx1*. Alignments to chr10:102498500-102455000 mouse genomic sequences (July 2007/mm9 assembly) were performed using the UCSC Genome Browser (Kent et al., 2002). The conserved genomic regions analyzed by ChIP, their sizes and positions are indicated in red. **(B)** ChIP of Emx2 or Pbx binding to genomic sequences spanning *Alx1*. The graph represents the average enrichment of control antibody (white), Emx2-bound (light gray) or Pbx-bound (dark gray) *Alx1* genomic regions, as assessed by semi-quantitative PCR. Values indicate the percentage ratio between DNA amounts in immunoprecipitates (IP) and input chromatin. Error bars represent the mean percentage IP/input ratio ± s.e.m. of at least three independent ChIPs for each sample. **(C)** Interspecies alignment of a 54 bp sequence (*Alx1*-EPBS) within the *Alx1* 5'-7 region containing possible Emx2-Pbx binding sites. TGAT (Site A) and TCAT (Site B) core motifs are in gray. Two non-conserved ATTA motifs (Site C) are underlined. **(D)** Emx2 and Pbx1 cooperatively bind the *Alx1*-EPBS sequence via the TGAT and TCAT motifs. EMSA using the *Alx1*-EPBS, or the EPBS-Amut, EPBS-Bmut and EPBS-Cmut oligonucleotides as probes. Black arrow indicates the Emx2-Pbx1 heterodimer; gray arrow indicates a retarded complex formed by Pbx1 alone; white arrows indicate the supershifted Emx2-Pbx1 complexes. **(E)** Luciferase activity, in arbitrary units, assayed from P19 cells transiently transfected with the pML*Alx1*-EPBS(900) [EPBS(900)] or pML*Alx1*-EPBS (EPBS) reporters, or their mutated derivatives [EPBS(900)A+Bmut, EPBS-Amut, EPBS-Bmut, EPBS-Cmut] together with Pbx1 and/or Emx2 expression constructs. Bars represent mean luciferase activity ± s.e.m. of at least four independent experiments.

Pbx factors hierarchically control genes crucial for scapular blade development including *Emx2*, which, in turn, regulates blade progenitor cell proliferation

In mice, *Emx2*⁻/⁻ embryos do not initiate mesenchymal condensation in pre-blade domains (Pellegrini et al., 2001), and in chick *Emx2* functions upstream of *Sox9* (Huang et al., 2006). *Emx2* has thus been considered to maintain the positional identity of cells fated to form the blade (Bi et al., 2001; Prols et al., 2004). Here, we reveal that *Emx2* controls cell proliferation in the pre-blade mesenchyme. Thus, the reduction of *Sox9* and absence of the blade observed in *Emx2*⁻/⁻ mutants (Pellegrini et al., 2001) might be partially due to this perturbed cellular behavior.

In Pbx1/2Mut forelimbs, *Emx2* expression was severely reduced (Fig. 1B) and *Sox9* expression was diminished across the pre-blade region, as shown by OPT (Fig. 3). Similar, although not as extreme,

reductions were observed in Pbx1/3Mut domains (Fig. 3). These data suggest that Pbx genes cooperate and genetically regulate *Emx2* (and *Sox9*). Interestingly, unlike *Emx2⁻/⁻* embryos, Pbx1/2Mut embryos did not exhibit proliferation defects. It remains unclear how *Emx2* dosage influences cell proliferation, as *Emx2⁺/⁻* embryos retain normal cell proliferation (data not shown) and intact blades. Similarly, *Emx2*, although reduced in Pbx1/2Mut embryos, might still be present at sufficient levels to sustain cell division. Alternatively, the compound absence of all three Pbx genes might be required for the complete loss of *Emx2* expression (Fig. 8B) and reduction of cell proliferation.

Pbx genes also control a second pathway involved in blade patterning, which includes *Alx1/Alx4*, *Gli3*, and *Tbx15*, genes that have specific roles in patterning the superior, central, and inferior blade domains, respectively (Fig. 8B) (Kuijper et al., 2005). From E10-11, they become co-expressed with *Emx2* in the proximal limb and somatopleure, within a region fated to form the scapula (Huang et al., 2006). A seminal study (Kuijper et al., 2005) demonstrated that blade patterning is sensitive to gene dosage, with the most extreme reductions occurring when *Tbx15* loss is coupled with reduced dosage of either at least one gene crucial for inferior blade patterning (i.e. *Gli3*), or of at least two genes essential for superior blade patterning (e.g. *Alx1* and *Alx4*). We observed that the expression of these genes in *Pbx1⁻/⁻*, Pbx1/2Mut and Pbx1/3Mut embryos is disrupted proportionally to the severity of blade defects in each respective mutant and that such abnormalities occur without detectable perturbations in cell proliferation or apoptosis (Fig. 8A). Accordingly, at E10.5, the expression of all known blade-patterning genes was reduced to nearly undetectable levels in Pbx1/2Mut, whereas only a subset of these genes (*Alx1*, *Alx4* and *Gli3*) was altered in Pbx1/3Mut, and, lastly, only *Alx1* was modestly reduced in *Pbx1⁻/⁻* mutants (Fig. 5). Of interest, Pbx1/3Mut embryos additionally exhibit foramina, a phenotype resembling that reported in *extra toes* (*Gli3*) (Hui and Joyner, 1993; Johnson, 1967; Schimmang et al., 1992) and polycomb gene *M33⁻/⁻* (*Cbx2* – Mouse Genome Informatics) (Core et al., 1997) mutant mice. Accordingly, Pbx genes have been shown to mediate polycomb expression in axial mesodermal tissues (Capellini et al., 2008).

Pbx1 is an interaction partner of Emx2 in scapular blade development

Our studies reveal that, unlike *Pbx1-3*, whose domains of genetic interaction include blade and head regions, *Pbx1* and *Emx2* interaction is restricted to the blade. Compound *Pbx1⁺/⁻;Emx2⁺/⁻* and *Pbx1⁻/⁻;Emx2⁺/⁻* (Pbx1/Emx2Mut) mutants exhibit novel blade defects (i.e. proximal indentations and blade bifurcations) that are absent from single *Pbx1⁺/⁻*, *Pbx1⁻/⁻*, *Emx2⁺/⁻* or *Emx2⁻/⁻* embryos (Fig. 2) and are likely to arise from reductions in *Sox9*-positive cells along the vertebral border of the blade. These defects are partially mediated by Emx2 control of cell proliferation, as documented in blade-forming domains of Pbx1/Emx2Mut embryos. Although one copy of *Emx2* is present in the latter genotype and *Pbx1⁻/⁻* embryos lack changes in *Emx2* expression, decreased levels of *Emx2* might be sufficient to cause proliferation defects. Thus, the bifurcation and substantial blade loss in Pbx1/Emx2Mut embryos might be a partial consequence of reduced mesenchymal cell number and condensations.

Importantly, analyses of Pbx1/Emx2Mut embryos also showed that *Pbx1* and *Emx2* cooperatively control genes upstream of superior blade patterning (*Alx1* and *Alx4*) (Fig. 8B). Concomitantly, they might govern genes patterning other blade domains, as
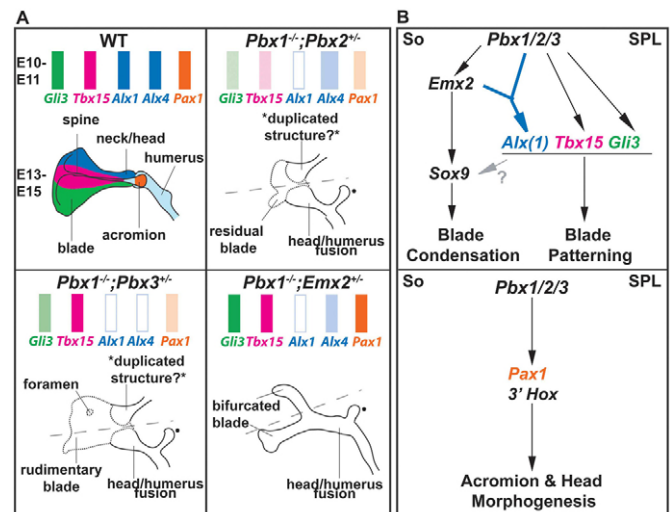

Fig. 8. Pbx and Emx2 interaction and function in scapular development. (**A**) Summary of marker gene expression for blade and spine (top) and of phenotypes (bottom) in each compound Pbx and *Pbx1;Emx2* mutant. Colored rectangles (top) at E10-11 depict normal expression levels and domains for genes specifying superior-to-inferior blade and acromial structures, color-coded in the E13-15 WT scapula (bottom). Lighter/unshaded rectangles depict reduced/nearly absent expression levels, and wider rectangles indicate expanded domains. Specific phenotypes for each mutant are represented versus WT (bottom). Changes in gene expression versus WT underlie the respective reductions in blades and spines in each mutant. A filled dot indicates what is most likely to be a malformed coracoid process. (**B**) Model of Pbx and Emx2 function in scapular development. (Top) Hierarchical genetic relationships between *Pbx1-3*, *Emx2*, *Sox9* and blade markers in scapular blade condensation and patterning in the somatopleure (So) and superior proximal limb (SPL). A bifurcated blue arrow indicates that Pbx1 and Emx2 genetically and biochemically interact to regulate *Alx1* transcription. It remains unknown whether blade-patterning genes control condensation and chondrogenesis (gray arrow with question mark). (Bottom) Pbx function upstream of *Pax1* and acromion morphogenesis and of 3′ Hox gene and head morphogenesis within the So and SPL.

Emx2⁻/⁻ and compound Pbx1/2Mut embryos lack *Tbx15* expression (Fig. 5; see Fig. S3 in the supplementary material). However, owing to in utero lethality of *Pbx1⁻/⁻;Pbx2⁺/⁻* mutants, the generation of more complex *Pbx1-3;Emx2* genotypes was impossible.

We also uncovered that Pbx1 and Emx2 heterodimerize at specific DNA sequences. Indeed, the Emx2 homeodomain YPWL motif (Bürglin, 1994), which is identical to part of the 'hexapeptide' required for Hox-Pbx interaction (reviewed by Moens and Selleri, 2006), is likely to mediate Emx2-Pbx1 heterodimerization. We found that the Emx2-Pbx1 heterodimer preferentially binds the CTTTAATGAT sequence (EP site), within which TGAT represents the Pbx1 half-site (Lu et al., 1995; Van Dijk et al., 1993). Interestingly, the tandem half-site configuration bound by Emx2-Pbx1 differs from that adopted by Hox-Pbx heterodimers, whereby Hox occupies a half-site 3′ to the TGAT Pbx1 binding sequence (Chang et al., 1996). This difference is not due to a TGAT position bias in the oligonucleotide used in site selection because a similar oligonucleotide, containing random nucleotides at five positions 3′ to the TGAT, did not promote Emx2-Pbx1 heterodimer binding (not shown).

Alx1, a regulator of scapular blade formation, is a target of Pbx and Emx2 factors

Among the *aristaless*-related genes involved in scapular development, *Alx1* has a pre-eminent function (Kuijper et al., 2005). Expression of *Alx1*, loss-of-function of which results in superior blade defects (Kuijper et al., 2005), was undetectable in Pbx1/2Mut, Pbx1/3Mut and Pbx1/Emx2Mut embryos (Fig. 5A, left). *Alx1* loss occurred in the absence of cell proliferation and apoptosis defects in Pbx1/2Mut embryos, whereas it was accompanied by a decrease in cell proliferation in Pbx1/Emx2Mut embryos. Interestingly, in *Emx2*$^{-/-}$ embryos, which exhibit blade loss and a marked decrease in cell proliferation, part of the *Alx1* expression territory was maintained. Overall, these data strongly suggest that Pbx and Emx2 factors are required for *Alx1* transcription. Indeed, we identified a conserved element (*Alx1* 5′-7) upstream of the putative *Alx1* TSS that is bound in vivo by Emx2-Pbx1, suggesting that both proteins directly control *Alx1* expression in pre-scapular domains. Although the possibility cannot be excluded that other sites more distant from *Alx1* might recruit Emx2 and/or Pbx1, we did not detect additional binding by Emx2-Pbx1 within the 16 evolutionarily conserved regions that were analyzed, covering more than 25 kb around *Alx1*. Interestingly, the *Alx1* 5′-7 element lacks a DNA sequence identical to the EP site, but displays two nearby conserved motifs that are both required for cooperative Emx2-Pbx1 binding. Of these, one contains the TGAT Pbx half-site (Site A), and the other a TCAT motif (Site B), which is also present within the selected EP site (complementary strand). Additionally, other predicted Pbx1 and Emx2 sites within the conserved element are not bound by their respective proteins as assayed by EMSA. The *Alx1*-EPBS element furthermore mediated transactivation in transient transfections of cultured cells only when Emx2 and Pbx1 were co-expressed. Interestingly, whereas mutation of the TGAT (Site A) or the TCAT (Site B) motif alone within the *Alx1*-EPBS element caused a discrete decrease in Emx2-Pbx1-mediated transactivation, only the compound mutation of both motifs significantly reduced reporter activity, underscoring that both Sites A and B are necessary for full transcriptional activation by Emx2-Pbx1.

In conclusion, here we have addressed the hierarchical control of scapula development by Pbx genes and their interaction with *Emx2*. We have uncovered that Pbx genes act upstream of head development and control genetic pathways underlying blade formation (Fig. 8B) (Kuijper et al., 2005). Importantly, we have established that Pbx genes hierarchically control *Emx2* and blade mesenchymal condensation, and that Pbx1 and Emx2 genetically and physically interact in blade patterning. Lastly, by highlighting a direct synergistic regulation of *Alx1* by Pbx1-Emx2, we have delineated a novel genetic network underlying shoulder girdle development.

Competing interests statement
The authors declare no competing financial interests.

Supplementary material
Supplementary material for this article is available at
http://dev.biologists.org/lookup/suppl/doi:10.1242/dev.048819/-/DC1

References
Aubin, J., Lemieux, M., Tremblay, M., Berard, J. and Jeannotte, L. (1997). Early postnatal lethality in Hoxa-5 mutant mice is attributable to respiratory tract defects. *Dev. Biol.* **192**, 432-445.

Aubin, J., Lemieux, M., Tremblay, M., Behringer, R. R. and Jeannotte, L. (1998). Transcriptional interferences at the Hoxa4/Hoxa5 locus: importance of correct Hoxa5 expression for the proper specification of the axial skeleton. *Dev. Dyn.* **212**, 141-156.

Aubin, J., Lemieux, M., Moreau, J., Lapointe, J. and Jeannotte, L. (2002). Cooperation of Hoxa5 and Pax1 genes during formation of the pectoral girdle. *Dev. Biol.* **244**, 96-113.

Beverdam, A. and Meijlink, F. U. (2001). Expression patterns of group-I aristaless-related genes during craniofacial and limb development. *Mech. Dev.* **107**, 163-167.

Bi, W., Huang, W., Whitworth, D. J., Deng, J. M., Zhang, Z., Behringer, R. R. and de Crombrugghe, B. (2001). Haploinsufficiency of Sox9 results in defective cartilage primordia and premature skeletal mineralization. *Proc. Natl. Acad. Sci. USA* **98**, 6698-6703.

Brendolan, A., Ferretti, E., Salsi, V., Moses, K., Quaggin, S., Blasi, F., Cleary, M. L. and Selleri, L. (2005). A Pbx1-dependent genetic and transcriptional network regulates spleen ontogeny. *Development* **132**, 3113-3126.

Bürglin, T. R. (1994). A comprehensive classification of homeobox genes. In *Guidebook to the Homeobox Genes* (ed. D. Duboule), pp. 25-72. Oxford, UK: Oxford University Press.

Capellini, T. D., Di Giacomo, G., Salsi, V., Brendolan, A., Ferretti, E., Srivastava, D., Zappavigna, V. and Selleri, L. (2006). Pbx1/Pbx2 requirement for distal limb patterning is mediated by the hierarchical control of Hox gene spatial distribution and Shh expression. *Development* **133**, 2263-2273.

Capellini, T. D., Zewdu, R., Di Giacomo, G., Asciutti, S., Kugler, J. E., Di Gregorio, A. and Selleri, L. (2008). Pbx1/Pbx2 govern axial skeletal development by controlling Polycomb and Hox in mesoderm and Pax1/Pax9 in sclerotome. *Dev. Biol.* **321**, 500-514.

Cartharius, K., Frech, K., Grote, K., Klocke, B., Haltmeier, M., Klingenhoff, A., Frisch, M., Bayerlein, M. and Werner, T. (2005). MatInspector and beyond: promoter analysis based on transcription factor binding sites. *Bioinformatics* **21**, 2933-2942.

Chalepakis, G., Fritsch, R., Fickenscher, H., Deutsch, U., Goulding, M. and Gruss, P. (1991). The molecular basis of the undulated/Pax-1 mutation. *Cell* **66**, 873-884.

Chang, C.-P., Shen, W.-F., Rozenfeld, S., Lawrence, H. J., Largman, C. and Cleary, M. (1995). Pbx proteins display hexapeptide-dependent cooperative DNA binding with a subset of Hox proteins. *Genes Dev.* **9**, 663-674.

Chang, C.-P., Brocchieri, L., Shen, W.-F., Largman, C. and Cleary, M. (1996). Pbx modulation of Hox homeodomain amino-terminal arms establishes different DNA-binding specificities across the *Hox* locus. *Mol. Cell. Biol.* **16**, 1734-1745.

Core, N., Bel, S., Gaunt, S. J., Aurrand-Lions, M., Pearce, J., Fisher, A. and Djabali, M. (1997). Altered cellular proliferation and mesoderm patterning in Polycomb-M33-deficient mice. *Development* **124**, 721-729.

Davidson, D., Graham, E., Sime, C. and Hill, R. (1988). A gene with sequence similarity to Drosophila engrailed is expressed during the development of the neural tube and vertebrae in the mouse. *Development* **104**, 305-316.

Depew, M. J., Liu, J. K., Long, J. E., Presley, R., Meneses, J. J., Pedersen, R. A. and Rubenstein, J. L. (1999). Dlx5 regulates regional development of the branchial arches and sensory capsules. *Development* **126**, 3831-3846.

Di Giacomo, G., Koss, M., Capellini, T. D., Brendolan, A., Popperl, H. and Selleri, L. (2006). Spatio-temporal expression of Pbx3 during mouse organogenesis. *Gene Expr. Patterns* **6**, 747-757.

Di Rocco, G., Mavilio, F. and Zappavigna, V. (1997). Functional dissection of a transcriptionally active, target-specific Hox-Pbx complex. *EMBO J.* **16**, 3644-3654.

Di Rocco, G., Gavalas, A., Popperl, H., Krumlauf, R., Mavilio, F. and Zappavigna, V. (2001). The recruitment of SOX/OCT complexes and the differential activity of HOXA1 and HOXB1 modulate the Hoxb1 auto-regulatory enhancer function. *J. Biol. Chem.* **276**, 20506-20515.

Fromental-Rain, C., Warot, X., Lakkaraju, S., Favier, B., Haack, H., Birling, C., Dierich, A., Doll, E. P. and Chambon, P. U. (1996). Specific and redundant functions of the paralogous Hoxa-9 and Hoxd-9 genes in forelimb and axial skeleton patterning. *Development* **122**, 461-472.

Garcia-Gasca, A. and Spyropoulos, D. D. (2000). Differential mammary morphogenesis along the anteroposterior axis in Hoxc6 gene targeted mice. *Dev. Dyn.* **219**, 261-276.

Huang, R., Zhi, Q., Patel, K., Wilting, J. and Christ, B. (2000). Dual origin and segmental organisation of the avian scapula. *Development* **127**, 3789-3794.

Huang, R., Christ, B. and Patel, K. (2006). Regulation of scapula development. *Anat. Embryol.* **211**, 65-71.

Hui, C. C. and Joyner, A. L. (1993). A mouse model of greig cephalopolysyndactyly syndrome: the extra-toes mutation contains an intragenic deletion of the Gli3 gene. *Nat. Genet.* **3**, 241-246.

Johnson, D. R. (1967). Extra-toes: a new mutant gene causing multiple abnormalities in the mouse. *J. Embryol. Exp. Morphol.* **17**, 543-581.

Kent, W. J., Sugnet, C. W., Furey, T. S., Roskin, K. M., Pringle, T. H., Zahler, A. M. and Haussler, D. (2002). The human genome browser at UCSC. *Genome Res.* **12**, 996-1006.

Kuijper, S., Beverdam, A., Kroon, C., Brouwer, A., Candille, S., Barsh, G. and Meijlink, F. U. (2005). Genetics of shoulder girdle formation: roles of Tbx15 and aristaless-like genes. *Development* **132**, 1601-1610.

Lu, Q., Knoepfler, P., Scheele, J., Wright, D. and Kamps, M. (1995). Pbx1 and E2A-Pbx1 bind the DNA motif ATCAATCAA cooperatively with the products of multiple murine Hox genes, some of which are themselves oncogenes. *Mol. Cell. Biol.* **15**, 3786-3795.

Matsuoka, T., Ahlberg, P. E., Kessaris, N., Iannarelli, P., Dennehy, U., Richardson, W. D., McMahon, A. P. and Koentges, G. (2005). Neural crest origins of the neck and shoulder. *Nature* **436**, 347-355.

McLeod, M. (1980). Differential staining of cartilage and bone in whole mouse fetuses by alcian blue and alizarin red S. *Teratology* **22**, 299-301.

Moens, C. B. and Selleri, L. (2006). Hox cofactors in vertebrate development. *Dev. Biol.* **291**, 193-206.

Oliver, G., De Robertis, E. M., Wolpert, L. and Tickle, C. (1990). Expression of a homeobox gene in the chick wing bud following application of retinoic acid and grafts of polarizing region tissue. *EMBO J.* **9**, 3093-3099.

Pellegrini, M., Pantano, S., Fumi, M. P., Lucchini, F. and Forabosco, A. U. (2001). Agenesis of the scapula in Emx2 homozygous mutants. *Dev. Biol.* **232**, 149-156.

Prahlad, K. V., Skala, G., Jones, D. G. and Briles, W. E. (1979). Limbless: a new genetic mutant in the chick. *J. Exp. Zool.* **209**, 427-434.

Prols, F., Ehehalt, F., Rodriguez-Niedenfuhr, M., He, L., Huang, R. and Christ, B. U. (2004). The role of Emx2 during scapula formation. *Dev. Biol.* **275**, 315-324.

Quandt, K., Frech, K., Karas, H., Wingender, H. and Werner, T. (1995). MatInd and MatInspector: new fast and versatile tools for detection of consensus matches in nucleotide sequence data. *Nucleic Acids Res.* **23**, 4878-4884.

Rancourt, D. E., Tsuzuki, T. and Capecchi, M. R. (1995). Genetic interaction between hoxb-5 and hoxb-6 is revealed by nonallelic noncomplementation. *Genes Dev.* **9**, 108-122.

Rhee, J. W., Arata, A., Selleri, L., Jacobs, Y., Arata, S., Onimaru, H. and Cleary, M. L. (2004). Pbx3 deficiency results in central hypoventilation. *Am. J. Pathol.* **165**, 1343-1350.

Ros, M. A., Lopez-Martinez, A., Simandl, B. K., Rodriguez, C., Izpisua Belmonte, J. C., Dahn, R. and Fallon, J. F. (1996). The limb field mesoderm determines initial limb bud anteroposterior asymmetry and budding independent of sonic hedgehog or apical ectodermal gene expressions. *Development* **122**, 2319-2330.

Salsi, V. and Zappavigna, V. (2006). Hoxd13 and Hoxa13 directly control the expression of the EphA7 ephrin tyrosine kinase receptor in developing limbs. *J. Biol. Chem.* **281**, 1992-1999.

Salsi, V., Vigano, M. A., Cocchiarella, F., Mantovani, R. and Zappavigna, V. (2008). Hoxd13 binds in vivo and regulates the expression of genes acting in key pathways for early limb and skeletal patterning. *Dev. Biol.* **317**, 497-507.

Schimmang, T., Lemaistre, M., Vortkamp, A. and Ruther, U. (1992). Expression of the zinc finger gene Gli3 is affected in the morphogenetic mouse mutant extra-toes (Xt). *Development* **116**, 799-804.

Selleri, L., Depew, M. J., Jacobs, Y., Chanda, S. K., Tsang, K. Y., Cheah, K. S., Rubenstein, J. L., O_Gorman, S. and Cleary, M. L. (2001). Requirement for Pbx1 in skeletal patterning and programming chondrocyte proliferation and differentiation. *Development* **128**, 3543-3557.

Selleri, L., DiMartino, J., van Deursen, J., Brendolan, A., Sanyal, M., Boon, E., Capellini, T., Smith, K. S., Rhee, J., Popperl, H. et al. (2004). The TALE homeodomain protein Pbx2 is not essential for development and long-term survival. *Mol. Cell. Biol.* **24**, 5324-5331.

Sharpe, J. (2003). Optical projection tomography as a new tool for studying embryo anatomy. *J. Anat.* **202**, 175-181.

Sharpe, J., Ahlgren, U., Perry, P., Hill, B., Ross, A., Hecksher-Sorensen, J., Baldock, R. and Davidson, D. (2002). Optical projection tomography as a tool for 3D microscopy and gene expression studies. *Science* **296**, 541-545.

Sharpe, P. T., Miller, J. R., Evans, E. P., Burtenshaw, M. D. and Gaunt, S. J. (1988). Isolation and expression of a new mouse homeo-box gene. *Development* **102**, 397-407.

Stankunas, K., Shang, C., Twu, K. Y., Kao, S. C., Jenkins, N. A., Copeland, N. G., Sanyal, M., Selleri, L., Cleary, M. L. and Chang, C. P. (2008). Pbx/Meis deficiencies demonstrate multigenetic origins of congenital heart disease. *Circ. Res.* **103**, 702-709.

Theil, T., Alvarez-Bolado, G., Walter, A. and Ruther, U. (1999). Gli3 is required for Emx gene expression during dorsal telencephalon development. *Development* **126**, 3561-3571.

Thompson, J. D., Higgins, D. G. and Gibson, T. J. (1994). CLUSTAL W: improving the sensitivity of progressive multiple sequence alignment through sequence weighting, position-specific gap penalties and weight matrix choice. *Nucleic Acids Res.* **22**, 4673-4680.

Tian, D. and Lev, S. (2002). Cellular and developmental distribution of human homologues of the Drosophilia rdgB protein in the rat retina. *Invest. Ophthalmol. Vis. Sci.* **43**, 1946-1953.

Timmons, P. M., Wallin, J., Rigby, P. W. and Balling, R. (1994). Expression and function of Pax 1 during development of the pectoral girdle. *Development* **120**, 2773-2785.

Van Dijk, M. A., Voorhoeve, P. M. and Murre, C. (1993). Pbx1 is converted into a transcriptional activator upon acquiring the N-terminal region of E2A in pre-B-cell acute lymphoblastoid leukemia. *Proc. Natl. Acad. Sci. USA* **90**, 6061-6065.

Wang, B., He, L., Ehehalt, F., Geetha-Loganathan, P., Nimmagadda, S., Christ, B., Scaal, M. and Huang, R. (2005). The formation of the avian scapula blade takes place in the hypaxial domain of the somites and requires somatopleure-derived BMP signals. *Dev. Biol.* **287**, 11-18.

Wilm, B., Dahl, E., Peters, H., Balling, R. and Imai, K. (1998). Targeted disruption of Pax1 defines its null phenotype and proves haploinsufficiency **95**, 8692-8697.

Wright, E., Hargrave, M. R., Christiansen, J., Cooper, L., Kun, J., Evans, T., Gangadharan, U., Greenfield, A. and Koopman, P. (1995). The Sry-related gene Sox9 is expressed during chondrogenesis in mouse embryos. *Nat. Genet.* **9**, 15-20.

Zappavigna, V., Sartori, D. and Mavilio, F. (1994). Specificity of HOX protein function depends on DNA-protein and protein-protein interactions, both mediated by the homeo domain. *Genes Dev.* **8**, 732-744.